

B₀-orientation dependent susceptibility-induced white matter contrast in the human brainstem

Manisha Aggarwal¹, Xu Li², Susumu Mori^{1,2}, and Peter C. M. van Zijl^{1,2}

¹Department of Radiology, Johns Hopkins University School of Medicine, Baltimore, MD, United States, ²F.M. Kirby Research Center, Kennedy Krieger Institute, Baltimore, MD, United States

Introduction: Recent evidence suggests that gradient echo (GRE)-based apparent relaxation rate (R_2^*) and phase mapping both exhibit modulation dependent on the orientation of white matter to the static B_0 field. While the origins of these effects are not completely understood yet, mechanisms proposed to explain the observed signal properties include magnetic susceptibility anisotropy^{1,2} and the generalized Lorentzian model for microscopic susceptibility inclusions³. In white matter, shaped perturbors associated with myelin microstructure have been implicated in the frequency shift and observed phase contrasts in GRE MRI. Investigation of the orientation-dependent modulation of GRE contrasts could thus potentially allow probing novel aspects of white matter microstructure, and yield insights into the biophysical mechanisms of the susceptibility-induced effects. Here, we investigate the B_0 -orientation dependence of quantitative R_2^* and signal frequency contrasts in the fixed human brainstem, which has a highly complex anatomy with orthogonal fiber populations. Our data reveal the generation of distinct tissue contrasts modulated by B_0 -field orientation. We further investigated direct estimation of fiber orientations based on the modulated R_2^* curves, and show close correspondence of the results to maps from diffusion MRI.

Methods: MR experiments were performed on an 11.7T Bruker NMR spectrometer using a 30-mm transceiver volume coil. 3D multi-gradient-echo data were acquired from a PFA-fixed human brainstem specimen (8 echoes, TE1=4 ms, interecho spacing 4 ms, TR=100 ms, bandwidth 100 kHz) at an isotropic resolution of $170 \times 170 \times 170 \mu\text{m}^3$. The brainstem axis was first oriented parallel (0°) to B_0 , and then rotated to 14 different orientations with respect to the B_0 field. For comparison, diffusion tensor (DTI) data were acquired at the same resolution, using a 3D-GRASE sequence (TE/TR=32/600 ms, b_0 +6 diffusion directions). Data were Fourier-transformed and R_2^* maps were fit orientation-wise by exponential least squares fitting to the multi-echo data. Images were spatially registered to the 0° data space using 3D transformation matrices derived by 12-parameter affine mapping. Phase data were processed by Laplacian unwrapping and spatially-filtered using V-SHARP⁴ to remove background fields. Frequency (f) maps were derived from filtered phase maps of the first and third echoes after scaling by $2\pi\text{TE}$. We used Levenberg-Marquardt nonlinear optimization to estimate the fiber orientations at each voxel via least squares fits of measured R_2^* and f values to generalized models $P=A\sin^4(\theta)+b$, where $g(\theta)$ was modeled as $\sin^4\theta$ and $\sin^2\theta$ for R_2^* and f , respectively⁵, and θ denotes the angle made by the estimated 3D fiber vector with B_0 . Fiber orientation maps were derived by scaling the estimated vector maps thus obtained by the fitted amplitude parameter A .

Results: R_2^* and frequency maps revealed distinct B_0 orientation-dependent tissue contrasts in the human brainstem. **Fig. 1** shows R_2^* and f maps at two orientations of the brainstem (0° and 89°) relative to B_0 . In the pons, longitudinal fascicles of the corticospinal tract (CST) interleave orthogonally between medio-laterally running transverse pontine fibers (TPF). At 0° , the CST fibers were parallel to B_0 and exhibited significantly ($p<0.001$) lower R_2^* values compared to pontine fibers perpendicular to B_0 (**Fig. 1A**). At 89° , this contrast was reversed, with a drastic increase ($p<0.001$) in R_2^* in the CST relative to the TPF, which in turn showed a corresponding decrease in R_2^* from 0° (**Fig. 1A'**). The inversion of the relative contrast between the two fiber groups can be distinctly seen in **Fig. 1**. Frequency maps at 0° (**Fig. 1B**) revealed negative frequencies for the CST compared to positive frequencies for the TPF, with a relative inversion of the two polarities observed at 89° (**Fig. 1B'**). The positive frequency shift in fibers perpendicular to B_0 is consistent with a more diamagnetic susceptibility effect. Plots of R_2^* and f as a function of angle of the brainstem axis with B_0 (**Fig. 1C**) indicated that the dependencies on B_0 -orientation closely approximated $\sin^4\theta$ and $\sin^2\theta$ curves, respectively (model fits to experimental data are shown by dashed lines). Further, the CST was found to exhibit a higher degree of peak-to-peak modulation of both R_2^* and f with B_0 -orientation, as quantified by the fitted amplitude parameter A for CST ($A=23.41 \text{ s}^{-1}$ for R_2^* and $+3.77 \text{ Hz}$ for f), compared to the TPF ($A=13.76 \text{ s}^{-1}$ for R_2^* and $+3.18 \text{ Hz}$ for f).

Fig. 2 shows the fitted A -map and estimated fiber orientation map derived from nonlinear least-squares fitting of the model to the multi-orientation R_2^* data. Maps in **Fig. 2B-C** demonstrate that interdigitating fiber orientations of the CST and TPF could be sensitively resolved based on contrast modulation of R_2^* with B_0 -orientation. The resulting orientation map showed close correspondence to the primary eigenvector map reconstructed from DTI (**Fig. 2A**).

Discussion & Conclusion: Our findings show that white matter fibers in the brainstem exhibit significant dependence of both R_2^* and frequency on their relative orientation to the static B_0 field, which closely approximate $\sin^4\theta$ and $\sin^2\theta$ dependent curves, respectively. Furthermore, the significantly higher amplitude of modulation of both R_2^* and f seen in the CST fibers compared to the TPF suggests that the underlying contrast mechanism can be potentially sensitive to differences in specific properties of tissue microstructure that affect its magnetic environment, e.g. myelin structure or density. These findings indicate that B_0 -orientation dependence of GRE frequency and magnitude data could potentially provide uniquely sensitive contrasts to probe white matter tissue orientation and microstructure in human nervous tissue.

References: [1] Liu 2010, MRM 63 [2] Lee *et al* 2010, PNAS 107 [3] Luo *et al* 2014, MRM 71 [4] Schweser *et al* 2012, *Nimg* 57 [5] Wharton & Bowtell, *Nimg* 83, 2013.

Acknowledgements: NIH grants R03EB017806, P41EB015909.

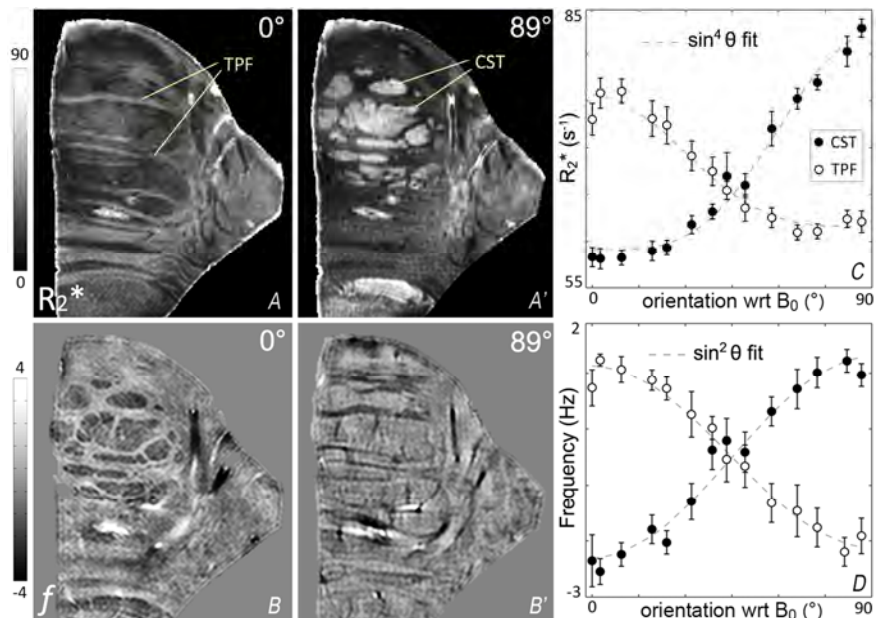


Fig. 1: B_0 -orientation dependent R_2^* and frequency contrasts in the brainstem. A-B) Comparison of R_2^* (A-A') and f (B-B') maps at two orientations (0° , 89°) relative to B_0 revealed distinctly inverted contrasts between corticospinal tract (CST) and transverse pontine fibers (TPF). CST fibers were prominently highlighted in the 89° R_2^* map, but could not be delineated at 0° . C) R_2^* and f in the CST and TPF plotted as a function of brainstem orientation relative to B_0 . Data indicate $\sin^4\theta$ and $\sin^2\theta$ modulations of R_2^* and f with B_0 -orientation, respectively (dashed lines show fits to the data).

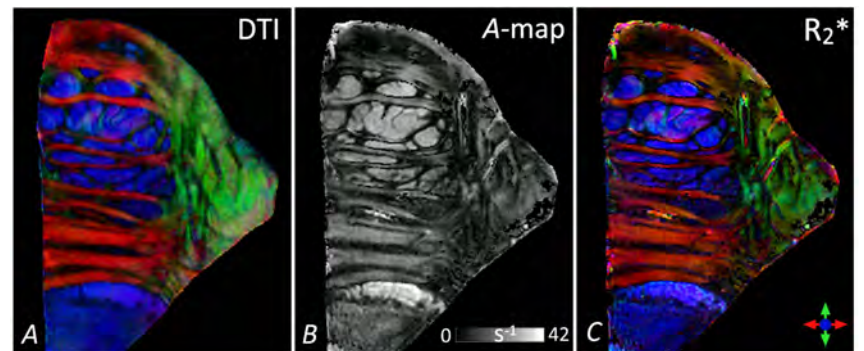


Fig. 2: A) Direction-encoded color map from DTI. B) Map of the fitted R_2^* amplitude parameter A , representing the degree of orientation-dependence of R_2^* . C) Fitted fiber orientation map estimated from the multi-orientation R_2^* data. Colors; red: left-right, green: top-down, blue: through-plane.